Automatic Video Analysis of Countermovement Jump Performance Using a Single Uncalibrated Camera

CHIU, Chuang-Yuan, CHANG, Chien-Chun, CHIANG, Yi-Chien and CHIANG, Chieh-Ying

Journal of Biomechanics 186 (2025) 112695

Contents lists available at ScienceDirect

Journal of Biomechanics

journal homepage: www.elsevier.com/locate/jbiomech

Automatic video analysis of countermovement jump performance using a single uncalibrated camera

Chuang-Yuan Chiu [a,*], Chien-Chun Chang [b,c,*], Yi-Chien Chiang [b], Chieh-Ying Chiang [d,e]

[a] Sports Engineering Research Group, Sport and Physical Activity Research Centre, Sheffield Hallam University, Sheffield, UK
[b] Graduate Institute of Athletics and Coaching Science, National Taiwan Sport University, Taoyuan, Taiwan
[c] Department of Sports Medicine, China Medical University, Taichung, Taiwan
[d] Department of Sports Training Science-Combats, National Taiwan Sport University, Taoyuan, Taiwan
[e] Taiwan Institute of Sports Science, Kaohsiung City, Taiwan

ARTICLE INFO

Keywords:
Computer vision
Machine learning
Biomechanics
Analysis
Testing

ABSTRACT

The countermovement jump (CMJ) assessment is widely employed for monitoring sports performance, traditionally relying on heavy and expensive force plates to extract performance variables like jump height and peak force. Inertial measurement unit (IMU)-based approaches and mobile applications have been developed to analyse CMJ performance with cost-effective devices, but they still require technical expertise and manual annotations during operation. We developed a new camera-based pipeline that can measure CMJ performance automatically by utilising computer vision techniques and biomechanical approaches from video captured by a single uncalibrated camera. Human segmentation and pose estimation techniques are used to understand the movement of the centre of mass and take-off and landing times. Combined with the biomechanical principles of object parabolic motion and inverse dynamics, the force–time data can be estimated for extracting CMJ performance variables. We recruited 77 elite athletes (29 females; height: 170.0 $\pm$ 9.0 cm; mass: 72.2 $\pm$ 17.7 kg) to evaluate the developed method against a commercial force platform. The developed method enables fully automatic CMJ analysis for both force–time data and performance variables from video captured by a camera without calibration. The results showed superior correlations ($R > 0.7$) and high reliability (%CV < 10 %) for most CMJ variables compared to the IMU-based approach. This approach automates CMJ analysis, offering more variables than existing mobile apps while reducing the technical demands of IMU-based methods. It streamlines assessment, making it ideal for large-scale cohort studies. Grounded in biomechanics, it enhances sports and health monitoring, enabling data-driven optimisation of human performance.

1. Introduction

The countermovement jump (CMJ) is a vertical jump initiated by a self-selected squat followed by a rapid leg extension (Bishop et al., 2021). The CMJ assessment is commonly used for testing and monitoring sports performance (Cormie et al., 2009). The CMJ utilises a stretch–shortening cycle (SSC) movement, which amplifies the muscle's pre-stretch state and enhances the subsequent force-generating capacity during the propulsion phase through various myogenic and neurogenic factors (Claudino et al., 2017; Laffaye et al., 2014; Ruffieux et al., 2020). Claudino et al. (2017) highlighted that the average jump height obtained from CMJ tests is a sensitive indicator for variations in neuromuscular status. In addition to assessing sports performance, CMJ tests are also widely used to measure training effects. Chang et al. (2022) examined the effects of judo training by employing both unloaded and loaded CMJ assessments. To ensure valid data for determining sports performance and training effects, an accurate and reliable measurement method is required.

Conventionally, force plates have been employed to capture ground reaction forces (GRFs) for force–time data, enabling performance variable extractions such as flight time as well as kinetic and kinematic variables, including jump height and peak force (Miranda-Oliveira et al.,

* Corresponding authors at: Advanced Wellbeing Research Centre, Sheffield Hallam University, Olympic Legacy Park, 2 Old Hall Road, Sheffield, S9 3TU, UK (C.-Y. Chiu), Department of Sports Medicine, China Medical University Campus Security Center Emergency, Taiwan. No. 100, Section 1, Jingmao Road, Beitun District, Taichung City 406040 Taiwan, R.O.C (C.-C. Chang).

E-mail addresses: c.chiu@shu.ac.uk (C.-Y. Chiu), jameschang@mail.cmu.edu.tw (C.-C. Chang), 1120321@ntsu.edu.tw (Y.-C. Chiang), markchiang@ntsu.edu.tw (C.-Y. Chiang).

https://doi.org/10.1016/j.jbiomech.2025.112695
Accepted 10 April 2025
Available online 12 April 2025

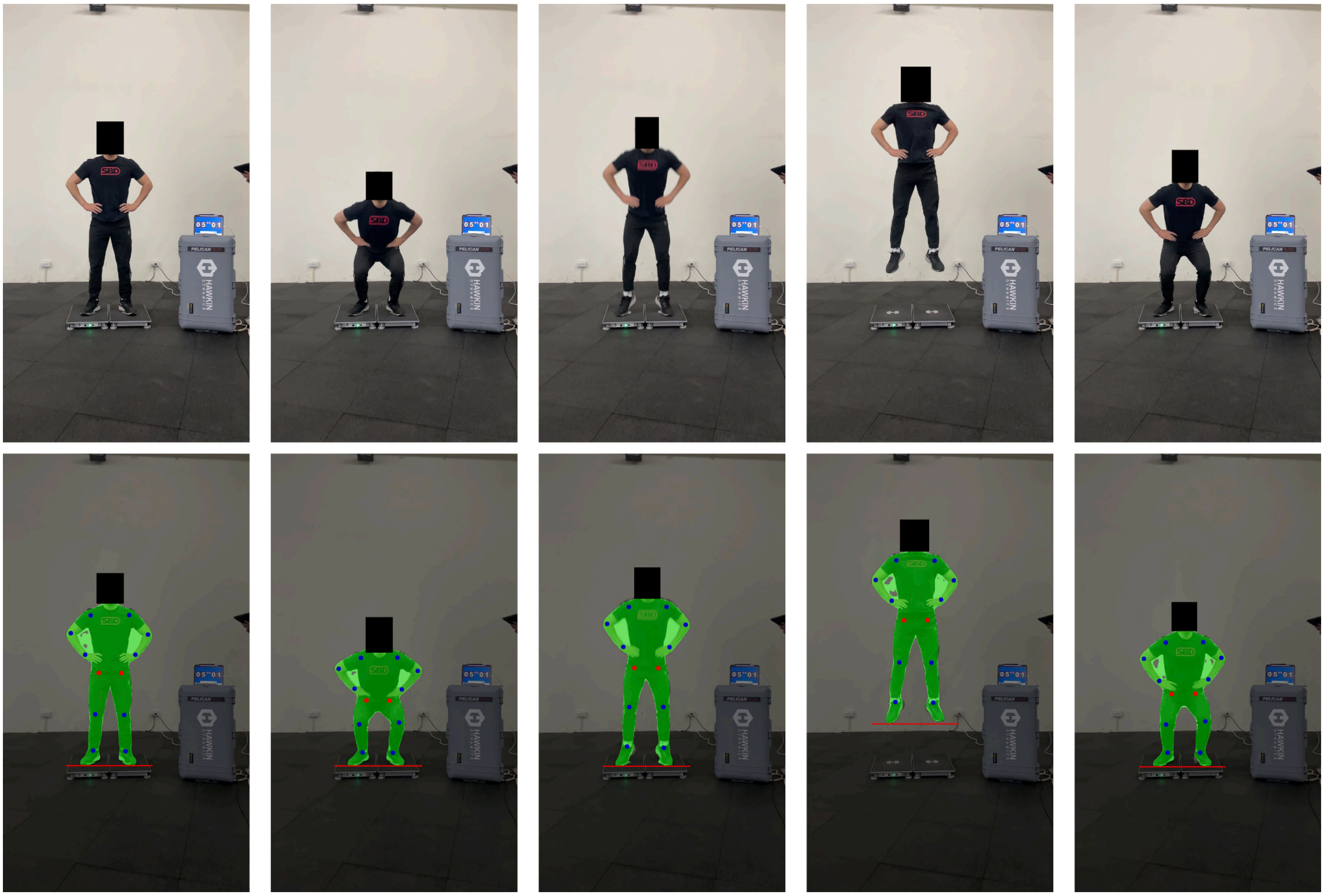

Fig. 1. Images captured by the mobile camera with the force plate setup (top row). The images were processed with computer vision techniques including pose estimation and human segmentation. The points represent the joints, and the red lines indicate the lower bound of the human segmentation. (For interpretation of the references to colour in this figure legend, the reader is referred to the web version of this article.)

2022; Toft Nielsen et al., 2019). Toft Nielsen et al. (2019) and Miranda-Oliveira et al. (2022) used force plates as a reference method for extracting performance variables to validate the estimation from inertial measurement units. Despite their capacity to provide accurate and high-frequency force values, force plates may not always be accessible (Mengarelli et al., 2018). This limitation has restricted their utilisation to specific teams and locations. Access to CMJ assessments using force plates is often limited for grassroots athletes and the general public because of their high cost (£30k − £70k) (Lake et al., 2018).

Recently, some manufacturers have introduced lightweight force platforms. Badby et al. (2023) and Lake et al. (2018) conducted validation studies on these lightweight force platforms compared to conventional systems. The measurements derived from the lightweight system exhibited good agreement with the results obtained from the conventional force platforms in both investigations (Badby et al., 2023; Lake et al., 2018), indicating small limits of agreement (LoA) and high correlations. However, the technique developed by Lake et al. (2018) typically requires a certain level of technical expertise for operation, including tasks such as exporting data and programming to extract CMJ performance variables. Furthermore, some lightweight systems remain expensive, costing around £10k–£15k (Lake et al., 2018), thereby still constraining their practicality for grassroots coaches and the general public.

Inertial Measurement Units (IMUs) have been used to measure acceleration and sensor location by placing the sensors on the trunk, near the centre of mass (CoM), enabling the prediction of force–time data and CMJ performance variables. Picerno et al. (2011) compared the CMJ height obtained from stereophotogrammetry and IMUs and found no significant difference between the two methods when trunk rotation was accounted for in the IMU results. Miranda-Oliveira et al. (2022) also used an IMU system to analyse CMJ performance and found that the IMU system could predict some variables with acceptable accuracy, such as flight time (95 % LoA less than ± 0.1 s compared to measurements from a force plate). However, accurate and precise data from IMUs require technical expertise to carefully place the sensors. Kerns et al. (2023) showed that inconsistent results in estimating force–time data from IMUs can be caused by varying sensor placements.

My Jump 2 and JumPo 2 are validated mobile applications (apps) that allow CMJ jump height measurement through a camera (Stanton et al., 2015; Vieira et al., 2023). The CMJ height measurements and modified reactive strength index (mRSI; defined as jump height divided by ground contact time) obtained from these apps have been compared with data obtained from conventional force plates (Balsalobre-Fernández et al., 2015; Bishop et al., 2022; Vieira et al., 2023). These studies highlight the potential of video analysis for obtaining accurate CMJ variable estimations. However, this kind of app requires manual annotation, which introduces small human errors into the analysis process. Balsalobre-Fernández et al. (2015) reported an inter-observer error of 0.1 ± 0.4 cm. The manual annotation procedure requires a meticulous frame-by-frame review of videos to precisely identify key time points such as take-off and landing, resulting in prolonged processing times. Additionally, the apps cannot provide force–time data. This limitation restricts their utility for kinetic data (e.g. peak force and jumping phase identification) in advanced sports performance analysis (McMahon et al., 2018).

Currently, no low-cost alternative to force plates efficiently provides

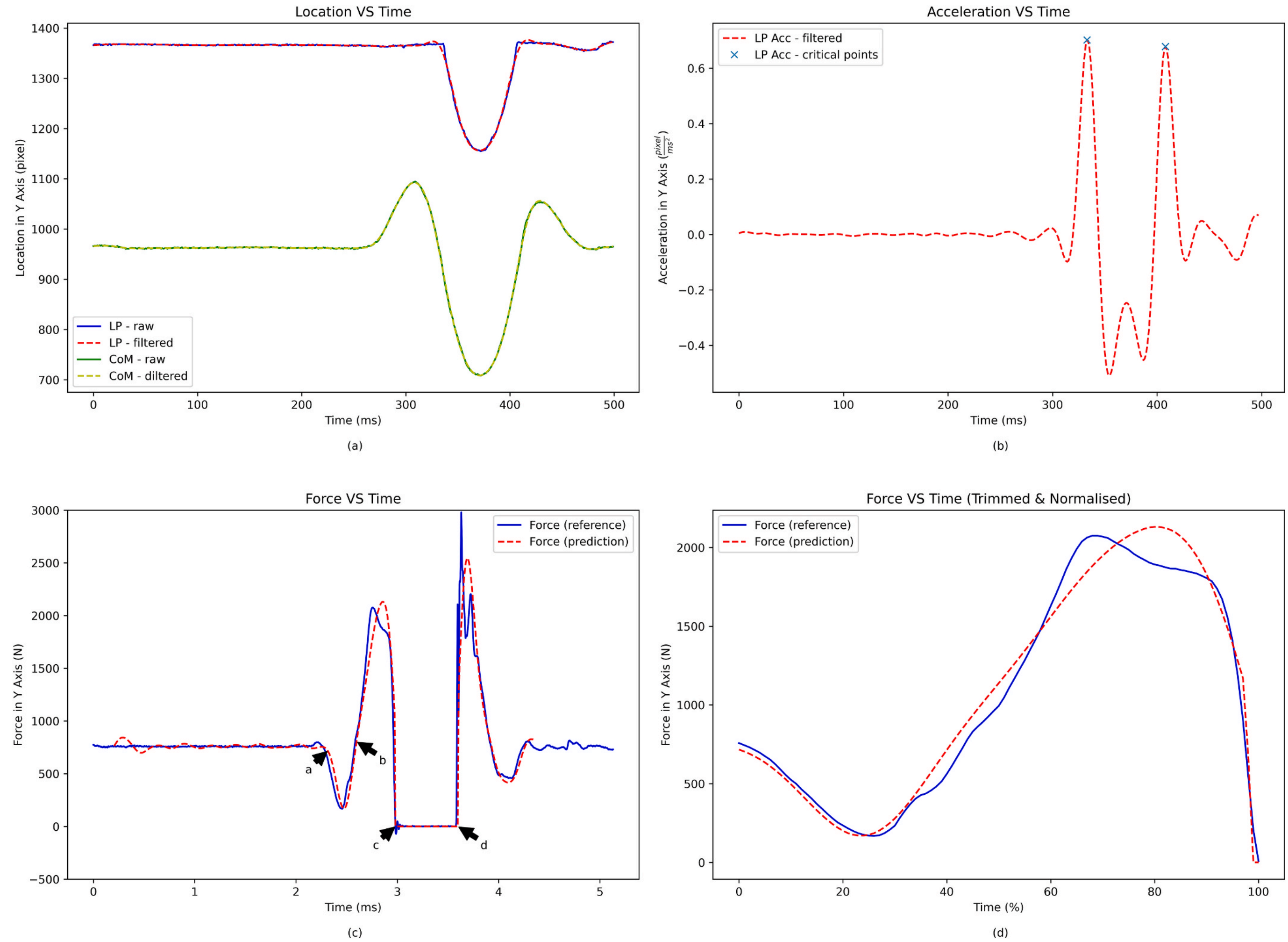

Fig. 2. Signal process in this study. (a) Butterworth low-pass filter was applied to smooth trajectories of the centres of mass (CoMs) and the lowest points of the human body (LPs). (b) The take-off and landing times were determined by the critical points (blue cross marks) of the LP acceleration (LP acc). (c) The reference and predicted force–time curves with the critical points for the instance of initiation of the jumping movement (point a), end of unweighting phase time and start of braking plus propulsion phase time (point b), take-off (point c) and landing (point d). The two curves were aligned with reference point c. (d) The reference and predicted force–time curves normalised between the instance of the jumping movement and the point of take-off. (For interpretation of the references to colour in this figure legend, the reader is referred to the web version of this article.)

force–time data and performance metrics. While low-cost force plates and IMUs show potential, they require technical expertise, forcing users to balance accuracy and practicality. Mobile apps offer limited data, which is insufficient for sports monitoring. Thus, there is a need for an affordable, accessible solution that accurately extracts force–time data and CMJ performance variables with minimal expertise.

Recently, computer vision has made significant advances through the adoption of deep learning techniques, including detection, segmentation, and pose estimation (Chen et al., 2019; MMPose Contributors, 2020). These advancements can complete tasks automatically without manual processing and have significantly reduced the post-processing time required for sports performance analysis (Papic et al., 2021). It can be hypothesised that computer vision methods could be used to analyse CMJ videos automatically for accurate and reliable GRF estimation. Nevertheless, these technologies have not been applied and validated for CMJ video analysis. The aims of this study are 1) to develop an automatic pipeline that uses computer vision techniques to obtain vertical GRFs and time data from a video captured by a single camera, and 2) to assess the accuracy and reliability of the developed pipeline by comparing it with a commercial force platform.

2. Methods

2.1. Participants

This study was approved by the university ethics committee (ER46859363). People with injuries that might affect CMJ performance were excluded. In total, 48 male (height: 174.3 ± 7.0 cm; mass: 76.3 ± 17.7 kg) and 29 female (height: 162.8 ± 7.0 cm; mass: 65.5 ± 15.8 kg) collegiate athletes from various sports were recruited (see supplementary material 1). All participants provided their informed consent for the conducted tests. They received regular sports training and CMJ assessment, so they were well-acquainted with the CMJ testing procedure. Participants wore appropriate clothing and footwear throughout the testing sessions.

2.2. Data collection

Each participant performed single CMJ tests (one jump per trial) with repeated trials. Data recording was accomplished using a commercial force platform (Hawkin Dynamics; 1000 Hz) in conjunction with a mobile phone camera (iPhone Apple iPhone 12 mini model A2176; 64 GB; iOS 17.1; frame rate: 120 Hz). Fig. 1 shows the images captured from the mobile phone during the CMJ test. The data collected from the Hawkin Dynamics system served as reference data in this study as its accuracy has been validated (Dos'Santos et al., 2024). The camera was positioned on a tripod at a height of around 120 cm in front of the participant, at approximately 2.5 m, to encompass the full CMJ movement. The camera axis was perpendicular to the participants' sagittal plane and avoided tilt. The capturing resolution of the mobile phone camera was 1920 $\times$ 1080 pixels.

Before performing CMJ, participants stood motionless, looking forward. They placed their hands on their hips with their right and left feet separately placed on the force plates. During the CMJ test, participants squatted to a self-selected depth and immediately executed a vertical jump (Bishop et al., 2021). Following this, both feet landed on the force platform. GRF data and video data were recorded.

2.3. Force plate data processing

Performance variables, including jump height, flight time, mRSI, contraction time, unweighting phase time, and peak force, were also extracted from the Hawkin Dynamics software via force plate measurements. The definition of these variables is listed on https://www.hawkindynamics.com/hawkin-metric-database. The braking plus propulsion phase time was calculated by subtracting the unweighting phase time from the contraction time. The minimum force during the unweighting phase was also recorded by adapting the Python scripts provided by Smith (2024).

The Hawkin Dynamics software was used to extract GRF data from the force plates. For comparison purposes, the force data were trimmed from the start of movement (unweighting phase start point) to the point of take-off and then normalised to 100 %. The take-off time point was identified as the first point where the vertical force was < 10 N (Smith, 2024), and the start of movement was determined by subtracting the contraction time from the take-off time point.

After processing the data from Hawkin Dynamics, the normalised force–time data and the following performance variables were obtained: peak force, minimum force, jump height, flight time, contraction time, braking plus propulsion (negative impulse) phase time, unweighting (positive impulse) phase time, and mRSI. The selection of performance variables was guided by a previous study (Miranda-Oliveira et al., 2022).

2.4. Video data processing

The videos captured by the mobile camera were saved in MOV format and processed at every frame and every 4th frame to simulate 120 fps and 30 fps data processing (see supplementary material 2 for the flow chart). Participant detection and segmentation in the videos were performed using PointRend (Kirillov et al., 2020), implemented through MMdetection (Chen et al., 2019). This choice of human segmentation algorithm was informed by promising outcomes in earlier research (Chiu et al., 2023). For joint localisation, the ViTPose algorithm (Xu et al., 2022) was integrated using MMPose (MMPose Contributors, 2020). ViTPose was a state-of-the-art approach with high accuracy across multiple datasets during this study. Fig. 1 shows an example of human segmentation and pose estimation in this study.

The CoMs were determined as the average positions of the left and right hip joints. The lowest points of the human body (LPs) were identified as the largest y-values among the segmented individuals within the provided images (i.e., human masks). To refine the trajectories of both CoMs and LPs, a 4th-order Butterworth low-pass filter with a 4 Hz cut-off frequency was applied as shown in Fig. 2(a). The filter setting is based on previous studies (Köklü et al., 2023; Sanders et al., 2015) due to the similar frame rates and movement characteristics (supplementary material 3).

The take-off and landing times were determined by the critical points of the LP acceleration, as shown in Fig. 2(b). The flight time can be calculated from the difference between these critical time points. The flight height (h) was derived directly from the period between the take-off and landing instances without determining image scale as shown in Equation (1).

$$h = \frac{1}{8} \times g \times (\mathit{flight\ time})^2 \tag{1}$$

The vertical velocity of CoM in the take-off moment ($v_{initial}$) can be estimated from the flight height by Equation (2).

$$v_{initial} = \sqrt{2 \bullet g \bullet h} \tag{2}$$

where g represents the acceleration due to gravity.

The velocity of CoMs before the take-off need to be estimated from pose estimation data for force–time data prediction. To achieve this, the image scaling in the vertical direction (r) was determined by the ratio of the pixel-based observation of the CoM take-off vertical velocity ($v_{initial}^{pixel}$) from the pose estimation results with the velocity estimated from the flight height ($v_{initial}$) by Equation (3).

$$r = \frac{v_{initial}^{pixel}}{v_{initial}} \tag{3}$$

The scaling factor (r) was subsequently used to compute the vertical velocity of CoMs and vertical acceleration of CoMs (a_{CoM}) with the pixel-based observation from the pose estimation results.

The estimation of vertical GRF ($\widehat{GRF}$) was predicted from the vertical acceleration of the CoMs and the participant's body mass (m_{body}) by using inverse dynamics as shown in Equation (4). When the participant was in the air, the $\widehat{GRF}$ was designated as 0 as shown in Fig. 2(c).

$$\widehat{GRF} = m_{body} \times (a_{CoM} - g) \tag{4}$$

After estimating $\widehat{GRF}$, the force–time data can be obtained.

The peak force was identified as the maximum force value before landing. The start of movement was defined as the point where the force dropped below 95 % of body weight, adapted from the definition by Hawkin Dynamics. Once the movement start time was established, the contraction time was calculated as the time difference between the movement start and take-off. The normalized force between the movement start and take-off was also calculated for comparison.

The boundary between the unweighting and braking plus propulsion phases was determined by the point of minimum velocity (McMahon et al., 2018). Once this boundary was confirmed, the unweighting and braking plus propulsion phase times and the mRSI were determined using the same method as for the Force Plate data. The minimum force was identified as the lowest force value during the unweighting phase. Fig. 2(c) illustrates an example of the estimated force with phase points marked. Fig. 2(d) shows the reference and predicted force–time curves normalised between the instance of the jumping movement and the point of take-off.

2.5. Statistical analyses

Mean absolute error (MAE), Pearson correlation coefficient (R), Bland and Altman analysis (Bland and Altman, 1999) and the effect size were selected to understand the accuracy of estimated force–time data and CMJ performance variables. Technical errors of measurement (TEM), coefficient of variation (%CV) and effect size were employed to quantify the absolute reliability of CMJ metric estimation for the developed pipeline. Additionally, the intraclass correlation coefficient (ICC) was used to quantify the relative reliability of CMJ metric estimation from the developed pipeline (see supplementary material 4 for acceptable thresholds).

Table 1
The descriptive statistics for the normalised force and CMJ metrics. (Reference = data extracted from force plates; mRSI = Modified Reactive Strength Index).

Metrics/Variables	mean ± std (reference)	mean ± std (120 FPS)	mean ± std (30 FPS)
Peak force (N)	1763.03 ± 433.01	1900.47 ± 475.87	1911.80 ± 470.18
Min force (N)	254.94 ± 152.48	294.80 ± 174.97	292.32 ± 174.86
Jump height (cm)	36.2 ± 7.4	38.2 ± 8.4	35.4 ± 8.0
Flight time (ms)	547 ± 60	555 ± 65	533 ± 65
Contraction time (ms)	808 ± 103	764 ± 105	750 ± 108
Unweighted phase time (ms)	371 ± 75	337 ± 79	336 ± 81
Braking plus propulsion phase time (ms)	438 ± 58	427 ± 65	414 ± 65
mRSI (m/s)	0.45 ± 0.11	0.51 ± 0.12	0.48 ± 0.12

3. Results

The proposed method enables automated CMJ analysis for both force–time data and performance variables extraction from camera-captured video, without requiring calibration for data collection and manual operation for data processing. The statistical characteristics of the performance variables are summarised in Table 1 (see supplementary material 5, 6 for normality test result and gender comparison).

Most performance variables estimated from 120 fps and 30 fps videos using the developed pipeline showed a high correlation (R > 0.7) with reference values obtained from the force platform (Table 2). The MAEs for force, peak force, and minimum force exceeded 50 N. Meanwhile, the MAEs for flight time, contraction time, unweighting phase time, and braking plus propulsion phase time were under 0.1 s. Most performance variables exhibited higher correlation coefficients when measured from 120 fps video compared to 30 fps.

The TEMs and %CVs for most performance variables, including peak force, minimum force, jump height, contraction time, and unweighting phase time, show better reliability when estimated from 120 fps videos than from 30 fps videos (Table 3). The %CV for minimum force (24.72 %) was notably higher than for other CMJ variables (<15 %). Additionally, ICCs for non-phase time performance variables were higher than those for phase time variables (i.e. contraction time, unweighting and braking plus propulsion phase time).

4. Discussion

The aims of this study were 1) to develop an automatic computer vision based pipeline to obtain vertical GRFs and time data from a video captured by a single camera, and 2) to compare the developed pipeline with the commercial force platform to determine their accuracy and reliability. In this study, we combined existing machine learning models with biomechanical principles to develop an automated pipeline for analysing jumping performance. The developed pipeline was compared with the force platform and showed good accuracy (R > 0.7; effect size < 0.63) and reliability for most CMJ variables (%CV < 10 %; ICC > 0.75). The data for this method were captured from a single camera without calibration, and the analysis processes were fully automatic. No

Table 2
Accuracy of ground reaction force and CMJ performance variables estimated from the developed pipeline and the IMU-based approach (Miranda-Oliveira et al., 2022). The 95 % confidence intervals were displayed in brackets beneath the metric values. (MAE = mean absolute error; *R* = Pearson correlation coefficient; Lower LoA = Lower bound of 95 % limit of agreement for Bland and Altman analysis; Upper LoA = upper bound of 95 % limit of agreement for Bland and Altman analysis).

Metrics/Variables	MAE (120 FPS)	*R*(120 FPS)	Lower LoA (120 FPS)	Upper LoA (120 FPS)	Effect Size (120 FPS)	MAE (30 FPS)	*R*(30 FPS)	Lower LoA (30 FPS)	Upper LoA (30 FPS)	Effect Size (30 FPS)	MAE (IMU)	LoA (IMU)	*R*(IMU)
Force (N)	160.09	0.94	−402.07	433.15	0.07	222.66	0.86	−650.97	612.33	−0.06	NA	NA	NA
	(157.87, 162.45)		(−408.85, −395.42)	(424.13, 441.06)	(0.05, 0.10)	(218.97, 226.44)		(−666.19, −636.15)	(601.09, 623.62)	(−0.09, −0.03)			
Peak force (N)	157.34	0.96	−137.31	412.18	0.98	171.32	0.95	−130.55	428.09	1.04	331	(−237.44, 797.44)	0.49
	(140.20, 176.72)		(−180.15, −96.09)	(367.39, 455.90)	(0.79, 1.17)	(153.86, 190.43)		(−175.02, −86.08)	(383.63, 472.56)	(0.85, 1.24)			
Min force (N)	91.88	0.74	−196.78	276.50	0.33	95.09	0.72	−205.15	279.90	0.30	76	(−201.16, 175.16)	0.76
	(77.58, 105.64)		(−260.07, −135.74)	(228.75, 318.36)	(0.05, 0.69)	(81.73, 109.46)		(−264.23, −149.07)	(235.36, 326.57)	(0.01, 0.65)			
Jump height (cm)	3.0	0.91	−4.8	8.8	0.57	2.6	0.88	−8.3	6.6	−0.22	4.0	(−8.704, 10.504)	0.71
	(2.6, 3.4)		(−7.0, −2.4)	(7.1, 10.2)	(0.19, 1.20)	(2.2, 3.1)		(−10.2, −6.3)	(5.1, 7.9)	(−0.46, 0.05)			
Flight time (ms)	17	0.92	−43	59	0.30	20	0.89	−71	44	−0.46	24	(−52.8, 64.8)	0.74
	(14, 20)		(−64, −20)	(42, 73)	(−0.02, 1.15)	(16, 24)		(−91, −49)	(29, 57)	(−0.71, −0.29)			
Contraction time (ms)	59	0.74	−191	103	−0.59	66	0.74	−208	92	−0.76	36	(−104.2, 72.2)	0.90
	(50, 70)		(−245, −146)	(70, 139)	(−0.89, −0.38)	(56, 78)		(−256, −163)	(62, 123)	(−1.09, −0.55)			
Unweighted phase time (ms)	56	0.60	−169	102	−0.48	57	0.57	−176	108	−0.47	55	(−125.72, 195.72)	0.23
	(48, 64)		(−195, −140)	(80, 123)	(−0.78, −0.24)	(49, 66)		(−206, −147)	(86, 127)	(−0.72, −0.24)			
Braking plus propulsion phase time (ms)	27	0.81	−86	65	−0.28	33	0.82	−96	48	−0.65	65	(−196.04, 94.04)	0.77
	(23, 32)		(−112, −65)	(47, 85)	(−0.55, −0.03)	(28, 37)		(−114, −81)	(37, 60)	(−0.95, −0.39)			
mRSI (m/s)	0.07	0.85	−0.08	0.18	0.80	0.05	0.82	−0.11	0.16	0.34	0.08	(−0.16, 0.21)	0.73
	(0.06, 0.07)		(−0.11, −0.05)	(0.16, 0.21)	(0.46, 1.21)	(0.05, 0.06)		(−0.14, −0.09)	(0.14, 0.19)	(0.08, 0.64)			

Table 3
Reliability of CMJ performance variables measured from the developed pipeline and the reference method (force plates). The 95 % confidence intervals are displayed in brackets beneath the metric values. (TEM = technical error of measurement; %CV = coefficient of variation; ICC = intraclass correlation coefficient; Reference = data obtained from force plates).

Metrics/Variables	TEM (120 FPS)	%CV (120 FPS)	ICC (120 FPS)	Effect Size (120 FPS)	TEM (30 FPS)	%CV (30 FPS)	ICC (30 FPS)	Effect Size (30 FPS)	TEM (Reference)	%CV (Reference)	ICC (Reference)	Effect Size (Reference)
Peak force (N)	120.62	6.35	0.94	0.32	126.78	6.63	0.94	0.37	86.47	4.90	0.96	0.14
		(3.05, 6.91)	(0.91, 0.96)	(−0.03, 0.66)		(3.17, 7.51)	(0.90, 0.96)	(0.06, 0.74)		(1.98, 6.75)	(0.94, 0.97)	(−0.24, 0.46)
Min force (N)	72.88	24.72	0.83	0.10	74.96	25.64	0.82	0.02	43.11	16.91	0.92	0.23
		(13.26, 24.57)	(0.74, 0.89)	(−0.13, 0.32)		(13.30, 25.52)	(0.72, 0.88)	(−0.21, 0.24)		(8.81, 17.03)	(0.88, 0.95)	(−0.00, 0.46)
Jump height (cm)	3.3	8.63	0.85	0.14	3.7	10.34	0.80	0.20	1.2	3.43	0.97	−0.09
		(3.35, 10.02)	(0.77, 0.90)	(−0.27, 0.46)		(4.22, 11.45)	(0.70, 0.87)	(−0.16, 0.56)		(1.96, 3.30)	(0.96, 0.98)	(−0.32, 0.14)
Flight time (ms)	28	5.07	0.82	0.12	32	6.00	0.76	0.17	11	2.00	0.97	−0.06
		(1.60, 6.23)	(0.73, 0.88)	(−0.22, 0.46)		(2.23, 7.09)	(0.65, 0.84)	(−0.17, 0.52)		(1.12, 1.95)	(0.95, 0.98)	(−0.28, 0.17)
Contraction time (ms)	61	7.99	0.66	−0.16	63	8.41	0.66	−0.18	53	6.54	0.74	−0.16
		(3.21, 10.91)	(0.52, 0.77)	(−0.49, 0.24)		(3.74, 10.71)	(0.52, 0.77)	(−0.53, 0.21)		(3.23, 6.92)	(0.62, 0.83)	(−0.56, 0.22)
Unweighting phase time (ms)	46	13.61	0.66	−0.06	55	16.40	0.53	−0.06	45	12.25	0.63	−0.08
		(6.52, 14.19)	(0.51, 0.77)	(−0.42, 0.36)		(8.05, 16.75)	(0.35, 0.68)	(−0.41, 0.37)		(6.05, 12.75)	(0.48, 0.75)	(−0.31, 0.15)
Braking plus propulsion phase time (ms)	36	8.50	0.70	−0.19	33	7.98	0.75	−0.26	23	5.28	0.84	−0.21
		(2.84, 12.63)	(0.56, 0.80)	(−0.53, 0.16)		(3.41, 10.00)	(0.64, 0.83)	(−0.60, 0.09)		(2.78, 5.31)	(0.76, 0.90)	(−0.44, 0.02)
mRSI (m/s)	0.05	9.26	0.86	0.22	0.05	11.35	0.81	0.25	0.03	7.25	0.90	0.11
		(4.53, 10.31)	(0.79, 0.91)	(−0.18, 0.59)		(5.72, 11.61)	(0.72, 0.87)	(0.01, 0.48)		(3.58, 7.83)	(0.85, 0.94)	(−0.27, 0.52)

sensor placement or manual operation is required for data collection or processing. This avoids the need for specialised knowledge to place the IMU sensors and manual annotation of the current mobile applications. This minimises the requirements of technical expertise and streamlines CMJ analysis. The developed pipeline can be an enhanced alternative to the current mobile application and IMU-based approaches for extensive cohort studies such as large sports performance surveys or regular training monitoring.

The developed pipeline leverages computer vision to automatically analyse CMJ videos, demonstrating good correlation and reliability (Pearson R: 0.91; ICC: 0.85) for jump heigh estimation, though slightly worse than the results from My Jump ($R > 0.95$; $ICC > 0.99$) as reported by Gençoğlu et al. (2023). The segmentation model in the developed pipeline occasionally introduces noise around the human boundary, leading to minor foot displacement; thus, a Butterworth filter is applied to smooth the trajectory. This filtering may introduce slight inaccuracies in detecting take-off and landing instances. However, the developed pipeline automates the analysis process, removing the need for manual annotation as required in My Jump 2 and JumPo 2, and can extract additional data, including force–time information and phase time variables. This approach not only minimises inter-observer error but also enhances data collection efficiency for large cohorts.

The developed pipeline demonstrated superior accuracy compared to IMU-based approaches. The developed pipeline showed stronger correlations with force platform reference data for most CMJ variables ($R > 0.8$) compared to IMU data ($R < 0.8$), as shown in Table 2 (Miranda-Oliveira et al., 2022). Additionally, the developed pipeline (120 fps) achieved narrower LoAs and lower MAEs for peak force, jump height, flight time, braking plus propulsion phase time, and mRSI than IMU-based methods (Table 2). The IMU sensor, attached to the skin, may experience prediction errors due to body deformation and muscle-damping effects, causing delays in phase identification. In contrast, the developed pipeline directly measures acceleration without sensor placement on the body. However, the low correlation for phase-related variables was likely due to pose estimation jitter affecting force predictions and start-time detection. The filter smooths jitter but may also eliminate small movements, leading to start-time detection errors. These issues may also contribute to lower ICC values for contraction time and phase times. Future research should explore advanced filtering strategies to enhance phase identification accuracy and reliability, enabling the method to serve as a viable alternative to portable force plates. Deep learning-based event detectors could improve accuracy by identifying key time points including start-time, take-off, and landing.

Apart from phase-related variables, the developed pipeline requires improvement in estimating minimum force (%CV = 24.72 %) to be a reliable alternative to force platforms (%CV = 17.06 %). The poor %CV of force platform suggests slight movement variations across repeated CMJ trials. The pose estimation model, trained using manual annotations, may not precisely align with hip anatomical landmarks, leading to random errors in the mid-hip position. These discrepancies, especially during the unweighting phase when the knee was bent, could introduce random error in CoM locations. Variations in pose and movement differences across trials may further impact consistency. Using a mid-hip CoM assumption cannot fully capture peak CoM acceleration, introducing random error in peak force estimation which lead to high MAE, effect size and wide LoA (Table 2). Future work should investigate more precise CoM estimation methods from human mesh recovery (Tripathi et al., 2023) to enhance the accuracy of force–time predictions.

When comparing results estimated with 120 fps versus 30 fps video, the higher frame rate shows small MAEs or higher correlations. This is expected, as more frames help reduce jitter issues of pose estimation and human segmentation when applying, allowing for more precise phase detection. For future applications, using the maximum possible frame rate is recommended to improve accuracy and precision. However, high frame rates (e.g. 1000 fps) demand significant hardware resources. To address this, machine learning-based frame rate upsampling techniques (Reda et al., 2022) should be explored and tested as a cost-effective alternative.

This study has several limitations. First, data from elite athletes may limit the generalizability to the general population, necessitating further testing. Second, the pipeline depends on specific camera settings, such as capture direction and resolution, which may affect accuracy. Future research should optimise these configurations. While computer vision models were trained on large datasets, variations in pose, body shape, background, and lighting could affect accuracy, requiring further validation in real-world scenarios. Additionally, inaccuracies in CoM estimation and phase detection should be addressed through advanced models like human mesh recovery and event detection. Users are advised to use the pipeline in simple backgrounds with proper lighting.

This study demonstrated that the developed pipeline, integrating computer vision, machine learning, and biomechanical techniques, can enhance existing mobile applications and IMU-based approaches. Sports scientists can use it to collect data outside the lab, enabling long-term monitoring of elite athletes who frequently travel for tournaments. Additionally, the pipeline has potential for healthcare applications, including home and clinical assessments. Streamlining data collection facilitates efficient cohort analysis of strength and conditioning variables, supporting data-driven interventions to optimise human performance.

5. Conclusions

In this study, we developed an automatic method to analyse countermovement jump (CMJ) videos captured by a camera without the need for calibration. Our findings demonstrate that our method enables a more accurate and reliable prediction of CMJ variables when compared to IMU-based approaches. Moreover, it offers supplementary information (vertical force–time data) that goes beyond what is currently accessible through existing mobile applications. This method holds significant potential as a valuable alternative to both mobile applications and IMU-based techniques, especially in large-scale cohort studies. Nevertheless, further enhancements in CMJ phase detection and CoM estimation are required to establish our method as a viable substitute for traditional force platforms.

CRediT authorship contribution statement

Chuang-Yuan Chiu: Writing – review & editing, Writing – original draft, Visualization, Software, Methodology, Formal analysis, Conceptualization. **Chien-Chun Chang:** Writing – review & editing, Writing – original draft, Validation, Supervision, Project administration, Methodology, Investigation. **Yi-Chien Chiang:** Data curation, Methodology, Project administration, Software, Writing – review & editing. **Chieh-Ying Chiang:** Conceptualization, Funding acquisition, Investigation, Methodology, Project administration, Resources, Software, Supervision, Validation, Writing – original draft, Writing – review & editing.

Declaration of Generative AI and AI-assisted technologies in the writing process

During the preparation of this work, the author(s) used ChatGPT and Gemini in order to enhance readability. After using this tool/service, the author(s) reviewed and edited the content as needed and take(s) full responsibility for the content of the publication.

Declaration of competing interest

The authors declare that they have no known competing financial interests or personal relationships that could have appeared to influence the work reported in this paper.

Acknowledgement

The authors acknowledge financial support from the Taiwan Institute of Sports Science (Grant No. TISS-2024-SS-03). The authors would like to thank the students who supported data collection for this study. For the purpose of open access, the author has applied a Creative Commons Attribution (CC BY) licence to any Author Accepted Manuscript version arising from this submission.

Appendix A. Supplementary material

Supplementary data to this article can be found online at https://doi.org/10.1016/j.jbiomech.2025.112695.

References

Badby, A.J., Mundy, P.D., Comfort, P., Lake, J.P., McMahon, J.J., 2023. The validity of Hawkin dynamics wireless dual force plates for measuring countermovement jump and drop jump variables. Sensors 23. https://doi.org/10.3390/s23104820.

Balsalobre-Fernández, C., Glaister, M., Lockey, R.A., 2015. The validity and reliability of an iPhone app for measuring vertical jump performance. J. Sports Sci. 33, 1574–1579. https://doi.org/10.1080/02640414.2014.996184.

Bishop, C., Berney, J., Lake, J., Loturco, I., Blagrove, R., Turner, A., Read, P., 2021. Bilateral deficit during jumping tasks: relationship with speed and change of direction speed performance. J. Strength Cond. Res. 35.

Bishop, C., Jarvis, P., Turner, A., Balsalobre-Fernandez, C., 2022. Validity and reliability of strategy metrics to assess countermovement jump performance using the newly developed smartphone application. J. Hum. Kinet. 83, 185–195.

Bland, J.M., Altman, D.G., 1999. Measuring agreement in method comparison studies. Stat Methods Med Res 8, 135–160. https://doi.org/10.1177/096228029900800204.

Chen, K., Wang, J., Pang, J., Cao, Y., Xiong, Y., Li, X., Sun, S., Feng, W., Liu, Z., Xu, J., 2019. MMDetection: Open mmlab detection toolbox and benchmark. arXiv preprint arXiv:1906.07155.

Chang, C.-C., Chen, T.-Y., Chia-Luan, Wu., Ho, P.-Y., Chiang, C.-Y., 2022. Effect of acute judo training on countermovement jump performance and perceived fatigue among collegiate athletes TI2 -. Int. J. Environ. Res. Public Health. https://doi.org/10.3390/ijerph192417008.

Chiu, C.-Y., Dunn, M., Heller, B., Churchill, S.M., Maden-Wilkinson, T., 2023. Modification and refinement of three-dimensional reconstruction to estimate body volume from a simulated single-camera image. Obes. Sci. Pract. 9, 103–111. https://doi.org/10.1002/osp4.627.

Claudino, J.G., Cronin, J., Mezêncio, B., McMaster, D.T., McGuigan, M., Tricoli, V., Amadio, A.C., Serrão, J.C., 2017. The countermovement jump to monitor neuromuscular status: a meta-analysis. J. Sci. Med. Sport 20, 397–402. https://doi.org/10.1016/j.jsams.2016.08.011.

Cormie, P., McBride, J.M., McCaulley, G.O., 2009. Power-time, force-time, and velocity-time curve analysis of the countermovement jump: impact of training. J. Strength Cond. Res. 23.

Dos'Santos, T., Evans, D.T., Read, D.B., 2024. Validity of the Hawkin dynamics wireless dual force platform system against a piezoelectric laboratory grade system for vertical countermovement jump variables. J. Strength Condition. Res. 38.

Gençoğlu, C., Ulupınar, S., Özbay, S., Turan, M., Savaş, B.Ç., Asan, S., İnce, İ., 2023. Validity and reliability of "My Jump app" to assess vertical jump performance: a meta-analytic review. Sci. Rep. 13, 20137. https://doi.org/10.1038/s41598-023-46935-x.

Kerns, J.A., Zwart, A.S., Perez, P.S., Gurchiek, R.D., McBride, J.M., 2023. Effect of IMU location on estimation of vertical ground reaction force during jumping. Front. Bioeng. Biotechnol. 11.

Kirillov, A., Wu, Y., He, K., Girshick, R., 2020. Pointrend: Image segmentation as rendering. In: Presented at the Proceedings of the IEEE/CVF conference on computer vision and pattern recognition, pp. 9799–9808.

Köklü, Ö., Alptekin, A., Korkmaz, H., 2023. Comparison of various devices used in the evaluation of vertical jump height. Pamukkale J. Sport Sci. 14. https://doi.org/10.54141/psbd.1332607.

Laffaye, G., Wagner, P.P., Tombleson, T.I.L., 2014. Countermovement Jump Height: Gender and Sport-Specific Differences in the Force-Time Variables. J. Strength Cond. Res. 28.

Lake, J., Mundy, P., Comfort, P., McMahon, J.J., Suchomel, T.J., Carden, P., 2018. Concurrent validity of a portable force plate using vertical jump force–time characteristics. J. Appl. Biomech. 34, 410–413. https://doi.org/10.1123/jab.2017-0371.

McMahon, J.J., Suchomel, T.J., Lake, J.P., Comfort, P., 2018. Understanding the key phases of the countermovement jump force-time curve. Strength Condition. J. 40.

Mengarelli, A., Verdini, F., Cardarelli, S., Di Nardo, F., Burattini, L., Fioretti, S., 2018. Balance assessment during squatting exercise: a comparison between laboratory grade force plate and a commercial, low-cost device. J. Biomech. 71, 264–270. https://doi.org/10.1016/j.jbiomech.2018.01.029.
Miranda-Oliveira, P., Branco, M., Fernandes, O., 2022. Accuracy of inertial measurement units when applied to the countermovement jump of track and field athletes. Sensors 22. https://doi.org/10.3390/s22197186.
MMPose Contributors, 2020. OpenMMLab Pose Estimation Toolbox and Benchmark. [WWW Document]. URL https://github.com/open-mmlab/mmpose.
Papic, C., Sanders, R.H., Naemi, R., Elipot, M., Andersen, J., 2021. Improving data acquisition speed and accuracy in sport using neural networks. J. Sports Sci. 39, 513–522. https://doi.org/10.1080/02640414.2020.1832735.
Picerno, P., Camomilla, V., Capranica, L., 2011. Countermovement jump performance assessment using a wearable 3D inertial measurement unit. J. Sports Sci. 29, 139–146. https://doi.org/10.1080/02640414.2010.523089.
Reda, F., Kontkanen, J., Tabellion, E., Sun, D., Pantofaru, C., Curless, B., 2022. Film: Frame interpolation for large motion. Presented at the European Conference on Computer Vision, Springer, pp. 250–266.
Stanton, R., Kean, C.O., Scanlan, A.T., 2015. *My Jump* for vertical jump assessment. Br. J. Sports Med. 49, 1157. https://doi.org/10.1136/bjsports-2015-094831.
Ruffieux, J., Wälchli, M., Kim, K.-M., Taube, W., 2020. Countermovement Jump training is more effective than drop jump training in enhancing jump height in non-professional female volleyball players. Front. Physiol. 11.
Sanders, R.H., Gonjo, T., McCabe, C.B., 2015. Reliability of three-dimensional linear kinematics and kinetics of swimming derived from digitized video at 25 and 50 Hz with 10 and 5 frame extensions to the 4th order Butterworth smoothing window. J. Sports Sci. Med. 14, 441.
Smith, J.C., 2024. Using python to analyze multiple countermovement vertical jumps over time. Strength Condit. J. 46.
Toft Nielsen, E., Jørgensen, P.B., Mechlenburg, I., Sørensen, H., 2019. Validation of an inertial measurement unit to determine countermovement jump height. Asia-Pacific J. Sports Med. Arthroscopy Rehabilitat. Technol. 16, 8–13. https://doi.org/10.1016/j.asmart.2018.09.002.
Tripathi, S., Müller, L., Huang, C.-H.P., Taheri, O., Black, M.J., Tzionas, D., 2023. 3D human pose estimation via intuitive physics. In: Presented at the Proceedings of the IEEE/CVF conference on computer vision and pattern recognition, pp. 4713–4725.
Vieira, A., Ribeiro, G.L., Macedo, V., de Araújo Rocha Junior, V., Baptista, R. de S., Gonçalves, C., Cunha, R., Tufano, J., 2023. Evidence of validity and reliability of Jumpo 2 and MyJump 2 for estimating vertical jump variables. PeerJ 11, e14558. Doi: 10.7717/peerj.14558.
Xu, Y., Zhang, J., Zhang, Q., Tao, D., 2022. Vitpose: Simple vision transformer baselines for human pose estimation. Adv. Neural Inf. Proces. Syst. 35, 38571–38584.